

- procedures for cylindrical aggregates gave 2×10^4 aggregates/mm² from a photomicrograph taken on a 0.2-mg diblock copolymer sample covering 5 cm². From this calculation, one gets 4.8×10^{-15} mol of diblock per aggregate or $N_0 = 3 \times 10^9$. In the case of PPQ₅₀-PS₃₀₀ aggregates containing 5 weight % solubilized C₆₀, 10^3 spherical aggregates/mm² were measured from a photomicrograph taken from a 0.2-mg diblock-C₆₀ sample covering 5 cm². From this information, one gets 9.6×10^{-15} mol of diblock per aggregate or $N_0 = 6 \times 10^9$. Similarly, for the case of aggregates containing 6 weight % C₆₀, $N_0 = 2 \times 10^{10}$.
18. S. A. Jenekhe *et al.*, *Chem. Mater.* **9**, 409 (1997).
 19. S. A. Jenekhe and J. A. Osaheni, *Science* **265**, 765 (1994).
 20. M. S. Dresselhaus, G. Dresselhaus, P. C. Eklund, *Science of Fullerenes and Carbon Nanotubes* (Academic Press, San Diego, CA, 1996).
 21. R. S. Ruoff, D. S. Tse, R. Malhotra, D. C. Lorents, *J. Phys. Chem.* **97**, 3379 (1993).
 22. N. Sivaraman *et al.*, *J. Org. Chem.* **57**, 6077 (1992).
 23. T. Andersson, K. Nilsson, M. Sundahl, G. Westman, O. Wennerstrom, *J. Chem. Soc. Chem. Commun.* **1992**, 604 (1992).
 24. J. L. Atwood, G. A. Koutsantonis, C. L. Raston, *Nature* **368**, 229 (1994).
 25. O. Ermer and C. Robke, *J. Am. Chem. Soc.* **115**, 10077 (1993).
 26. J.-M. Lehn, *Supramolecular Chemistry* (VCH, New York, 1995).
 27. G. M. Whitesides, J. P. Mathias, C. T. Seto, *Science* **254**, 1312 (1991).
 28. D. L. Wilcox Sr., M. Berg, T. Bernat, D. Kellerman, J. K. Cochran Jr., Eds., *Hollow and Solid Spheres and Microspheres: Science and Technology Associated with Their Fabrication and Application* (MRS Proc. 372, Materials Research Society, Pittsburgh, PA, 1995); S. Benita, Ed., *Microencapsulation: Methods and Industrial Applications* (Dekker, New York, 1996).
 29. D. M. Pai and B. E. Springett, *Rev. Mod. Phys.* **65**, 163 (1993); J. A. Osaheni, S. A. Jenekhe, J. Perlstein, *J. Phys. Chem.* **98**, 12727 (1994).
 30. We thank A. S. Shetty for helpful discussion and technical assistance. This research was supported by the Office of Naval Research and in part by the National Science Foundation (grants CTS-9311741 and CHE-9120001).

13 November 1997; accepted 2 February 1998

Inducing and Viewing the Rotational Motion of a Single Molecule

B. C. Stipe, M. A. Rezaei, W. Ho*

Tunneling electrons from the tip of a scanning tunneling microscope were used to induce and monitor the reversible rotation of single molecules of molecular oxygen among three equivalent orientations on the platinum(111) surface. Detailed studies of the rotation rates indicate a crossover from a single-electron process to a multielectron process below a threshold tunneling voltage. Values for the energy barrier to rotation and the vibrational relaxation rate of the molecule were obtained by comparing the experimental data with a theoretical model. The ability to induce the controlled motion of single molecules enhances our understanding of basic chemical processes on surfaces and may lead to useful single-molecule devices.

It is conceivable that, at the limit of miniaturization, individual atoms and molecules will physically constitute useful devices and their quantum properties will specify the desired functions and performance. A demonstration of such an atomic-scale electronic device was a reversible atomic switch that used a scanning tunneling microscope (STM) (1). In this experiment, a single Xe atom was transferred reversibly between the W tip of the STM and a Ni surface by the application of a voltage between them, resulting in bistable values of the tunneling current. A single-atom switch has also been demonstrated for Si adatoms on the Si(111)-7×7 surface where an atom was moved between two specific sites on the surface (2). The STM has been used to perform atomic-scale manipulation by a variety of other methods (3, 4), including the pushing or pulling of single atoms and molecules on a surface with the STM tip (5–8). By scanning regions of the Si(100)-(2×1) surface at high sample bias, it was possible to observe the reversible rotation of adsorbed Sb dimers between two stable orientations (9).

Using the basic method described in the atomic switch experiments (1, 2), we have studied the reversible rotation of single O₂ molecules among three equivalent orientations on the Pt(111) surface by accurately positioning the tip above the molecule and monitoring the rapid changes in tunneling current as the molecule rotates. Monitoring the tunneling current allows us to freeze the motion of the molecule in any chosen orientation and to compile statistics for the distribution of times spent in each orientation. The time dependence of the tunneling current yields a quantitative measure of the rotation rate and of the way in which this rate varies with the applied voltage and current. These studies show that the rotation is caused by the inelastic tunneling of low-energy electrons. The results provide insight into the adsorption and excitation properties of the molecule, including a value for the energy barrier to rotation.

The system O₂ on Pt(111) has been studied extensively because of the importance of Pt as a catalyst in oxidation reactions. Two chemisorbed O₂ species have been identified on Pt(111) below 100 K with the use of electron energy loss spectroscopy (EELS) (10, 11). The O–O bond for both species was determined by near-edge x-ray absorption fine structure spectroscopy to be aligned parallel or nearly

parallel to the surface (12). With the STM, we have recently identified the adsorption sites of these species and have discovered a third type at step edges (13). The subject of the present work is the species responsible for the 87-meV O–O stretch vibration observed in EELS (11). The STM images in Fig. 1 show these molecules as having a “pear” shape centered on the face-centered cubic (fcc), threefold hollow sites of the surface, with the bright lobe over a top site and the smaller, dimmer lobe over the opposite bridge site. By symmetry, they have three equivalent orientations separated by 120°.

Details of the homemade STM and experimental setup have been described elsewhere (14). We find the adsorption dynamics of O₂ on Pt(111) to be complex (13) because of the existence of a mobile precursor to chemisorption, whose lifetime and route to chemisorption are sensitive functions of temperature (14). In order to favor the adsorption of isolated O₂, the clean Pt(111) surface was exposed to O₂ at 85 K until a coverage of approximately 0.01 monolayer was observed. The surface was then cooled to 8 K to minimize temperature-induced effects. We rotated molecules by applying a voltage pulse to the sample while the tunneling current was recorded. Data shown in this report are for positive voltage pulses applied to the sample. An iterative tracking scheme was used to position the W tip at a chosen point above a molecule with lateral and vertical resolutions of 0.1 and 0.01 Å, respectively. We did this by searching out a local maximum or minimum of the tip height with the STM's feedback loop turned on to maintain constant tunneling current. Lateral offsets were added to give the desired tip position during the pulse. Feedback was then turned off, and the tip was moved vertically to give the desired initial current. The tip remained stationary during the voltage pulse.

After imaging an isolated O₂ molecule (Fig. 1A), we positioned the STM tip directly over the brightest point of the molecule where the tunneling current is at its

Laboratory of Atomic and Solid State Physics and Materials Science Center, Cornell University, Ithaca, NY 14853, USA.

*To whom correspondence should be addressed. E-mail: wilsonho@msc.cornell.edu

maximum for a given tip-surface separation. The voltage was then increased to a value that induces rotation, and the tunneling current was recorded. At the moment the molecule rotates, the tunneling current drops (Fig. 1B). A rescan of the same area shows that the molecule has rotated to one of the other two orientations (Fig. 1C). A repeat of the experiment shows the molecule in the third orientation (Fig. 1D).

Recent *ab initio* local-spin-density calculations are in quantitative agreement with both the vibrational energy and the observed STM image. The O–O bond axis was calculated to be tilted by 10° from the surface plane, with the O atom bonded toward the on-top site higher above the surface than the O atom bonded toward the opposite bridge site (15) (Fig. 2A). In general, as the molecule rotates under the tip, there will be three values of the tunneling current corresponding to the three energetically stable orientations of the molecule. As a result of symmetry, two values of the current will become

degenerate when the tip is positioned over the O–O axis. This is the case when the tip is located at the position of maximum tunneling current (labeled with a solid dot in Fig. 2B). Away from this axis, all three values of the tunneling current are visible during the voltage pulse (Fig. 2C). The computer could be instructed to end the voltage pulse at a particular value of the tunneling current, thus leaving the molecule in any desired orientation.

When the molecule was adsorbed next to a defect (impurity) site of the surface such as the one shown in the lower left of Fig. 1A, the molecule quickly returned to a preferred orientation during the voltage pulse (Fig. 2D). This was also the case when the molecule was adsorbed within a chain formation or island (13) and presumably results from a breaking in the threefold rotational symmetry of the potential energy surface.

The constraints in the rotation reveal the importance of local environmental ef-

fects. For consistency, we carried out detailed studies for isolated molecules with the tip positioned at the maximum current position. The measured times the molecule spent in the original (high-current) orientation were binned. The resulting distribution for a particular tunneling voltage and current was fitted to an exponential function (Fig. 3A). The molecule has no “memory” of the time it has spent in any particular orientation, and therefore an exponential distribution results from the constant rotation probability per unit time. The inverse of the exponential time constant gives the rotation rate, which has been determined as a function of tunneling current for various sample-tip voltages (Fig. 3B). A total of 21 isolated molecules were studied and rotated 1431 times to accumulate the data. For each voltage studied, the rotation rate was found to be proportional to I^N , where I is the tunneling current and N is a constant. The value of N depends on the sample bias voltage (Fig. 3C), and through modeling, this dependence is shown to reveal the mechanism for rotation.

Using the same theoretical model that successfully explained the current dependence of single-molecule dissociation rates (13), we propose that the mechanism for single-molecule rotation involves inelastic electron tunneling (scattering) by means of an adsorbate-induced resonance. The temporary occupation of this resonance with a tunneling electron corresponds to an electronically excited state of the molecule with a lifetime of a few femtoseconds. In each scattering process, energy is transferred to the hindered rotational mode of the molecule at a current-dependent rate. This vibrational excitation rate competes with a current-independent vibrational relaxation rate resulting from couplings to phonons and substrate electronic excitations. The maximum energy of the tunneling electrons is given by eV_{bias} , where e is the magnitude of the electron charge and V_{bias} is the bias voltage applied to the sample. If eV_{bias} is greater than the barrier to rotation, E_{rot} , the barrier can be overcome in one scattering event. This single-step process will dominate over multiple-step processes when the relaxation rate of the hindered rotation is much larger than the maximum electron tunneling rate (16). This is evidently the case here because the rotation rate depends linearly on current for sufficiently high sample bias.

The linearity also demonstrates that changes in the electric field have no significant effect on the rotation rate (the electric field increases as the tip-sample separation is reduced to supply more tunneling current). For $eV_{\text{bias}} < E_{\text{rot}}$, a ladder-climbing mechanism is involved wherein each

Fig. 1. (A) STM image of two “pear”-shaped O_2 molecules on fcc threefold hollow sites with one next to a defect. The sample was exposed to O_2 at 85 K and cooled to 8 K. (B) Current during a 0.15-V pulse over the isolated molecule in the center of the image showing the moment of rotation (step at $t \sim 20$ ms, where t is the time after the initiation of the pulse). (C) After-pulse image showing the second orientation of the molecule. (D) STM image taken after a second pulse with the molecule in the third orientation. The image in (A) was scanned at a tunneling current of 1 nA and a sample bias of 50 mV; images in (C) and (D) were scanned at 10 nA and 50 mV.

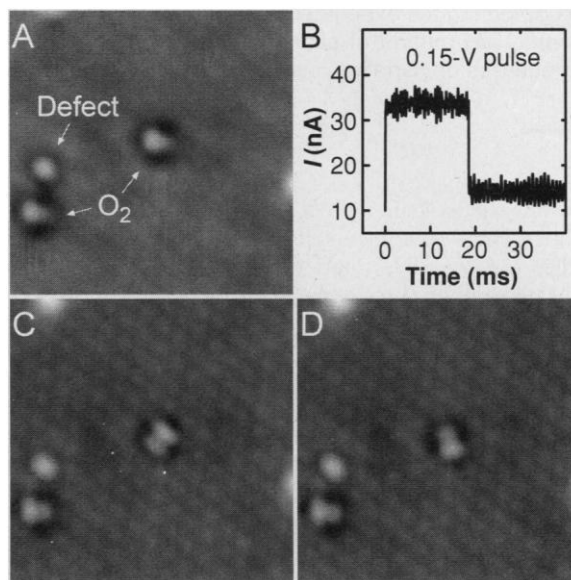
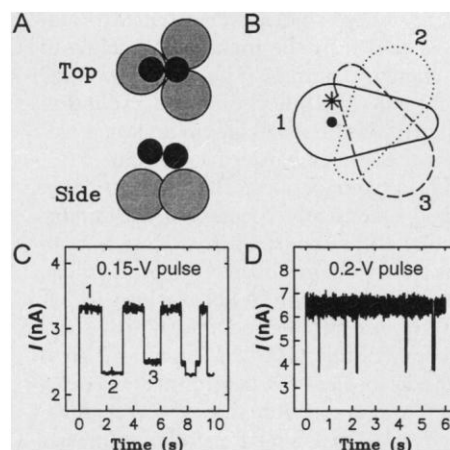


Fig. 2. (A) Schematic drawing showing top and side views of the fcc-site O_2 molecule (black circles); Pt atoms are shown in gray. (B) Schematic outline of “pear” molecule shape as seen in STM images for each orientation. The solid dot is the position of maximum tip height for the first orientation; this is the tip position used for data collection. The asterisk shows an off-axis tip position displaced 0.4 \AA from the solid dot. (C) Current during a 0.15-V pulse with the tip in the off-axis position in (B), showing three levels of current corresponding to the three orientations of the molecule. (D) Current during a 0.2-V pulse over a molecule next to an impurity showing a strong preference for a particular orientation.



scattering event promotes the molecule to a higher hindered rotational quantum state. Because of the short lifetime of the rotational state, the rotation rate is dominated by excitation processes that take the path with the least number of intermediate states that are energetically allowed. Each excitation rate is proportional to the tunneling current, and thus the overall rotation rate is proportional to I^N with N equal to the number of electrons needed to rotate the molecule. The energy barrier to rotation is then the highest eV_{bias} for which $N \geq 2$. From the exponent data in Fig. 3C we find $0.15 \text{ eV} < E_{\text{rot}} < 0.175 \text{ eV}$. Although only two electrons are necessary at 0.10 eV, the data show that both two-electron and higher electron processes contribute to the total rate because $N = 2.8$. This results in part from the quantized energy level structure of the potential well when no level exists near 0.10 eV. Also, the relaxation rate of the hindered rotation may not be much larger than the tunneling rate. When the tunneling current is larger than the relaxation rate, one would theoretically expect the rotation rate to become independent of voltage with N equal to the number of hindered rotation quantum states (17). The extrapolation of our data suggests that this occurs at about $I = 200 \text{ nA}$, giving an approximate value for the vibrational relaxation rate of $1.2 \times 10^{12} \text{ s}^{-1}$.

The midpoint of the O–O bond does not coincide with the center of the threefold hollow site. Calculations suggest that the molecule's midpoint and the threefold site's center are separated by 0.2 Å, with O₂ shifted toward the on-top site (15). Thus, the molecule does not execute a pure rota-

tion but shifts slightly as it rotates in the threefold hollow site. Furthermore, the molecule can eventually dissociate at the same voltages that induce rotation (Fig. 4A). The dissociation rates vary with tunneling current and voltage (13) but are generally much lower than the rotation rates. The limited

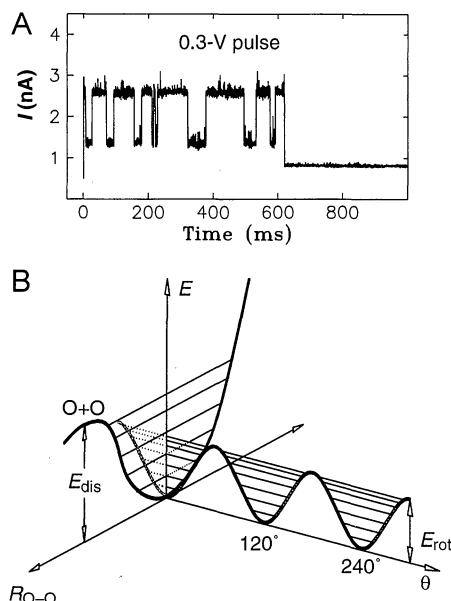
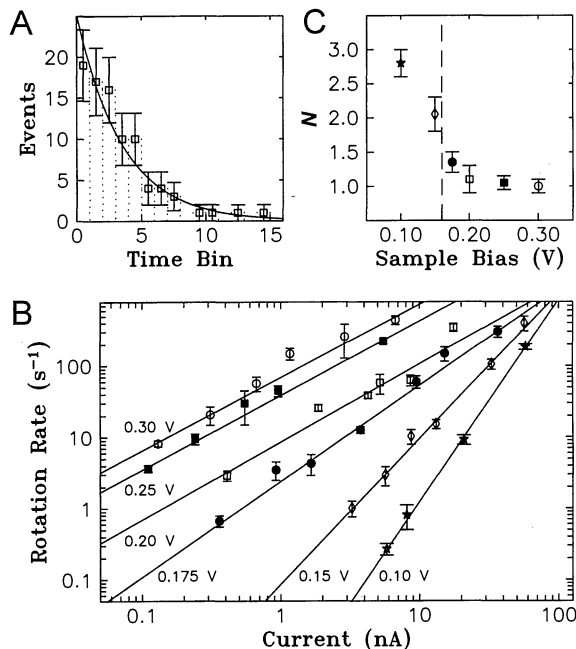


Fig. 4. (A) Tunneling current during a 0.3-V pulse above an isolated O₂ molecule. Rotation is followed by dissociation (step at $t \sim 610 \text{ ms}$). (B) Schematic of simple one-dimensional potential wells along the molecular stretch, $R_{\text{O-O}}$, and angular, θ , coordinates. Parallel lines in θ and $R_{\text{O-O}}$ directions are quantum levels of the hindered rotational mode and stretch mode, respectively (hindered rotational levels are likely to be more closely spaced than shown).

Fig. 3. (A) Example of a distribution of the times a single molecule spent in the high-current orientation with a fit to an exponential decay. A 0.2-V pulse was applied to the sample. The current was 1.9 nA when the molecule was in the high-current orientation (orientation 1 in Fig. 2B). The bin width is 12 ms. The analysis includes a total of 88 time intervals. Error bars are derived from Poisson statistics. (B) Rotation rate, R , as a function of tunneling current, I , for various applied biases. The solid lines are least-square fits to the data and correspond to power-laws, $R \propto I^N$. (C) A plot of N as a function of sample bias voltage. The dashed line denotes the bias voltage below which $N \geq 2$.



lifetime of the rotating O₂ as a result of dissociation implies that the potential-energy surface necessarily contains multidimensional pathways (Fig. 4B). Although the rotation involves the hindered rotational mode, the reaction coordinate for dissociation, $R_{\text{O-O}}$, corresponds to the O–O stretch mode and involves a different energy barrier, $E_{\text{dis}} \sim 0.38 \text{ eV}$. It is possible that there is a coupling between the two modes. If this coupling is sufficiently strong, rotation may be induced predominantly by initial excitation of the stretch mode. Also, the time spent by the molecule between stable orientations is too short to allow a determination of the orientation of the molecule at the moment of dissociation.

By inducing and viewing the controlled rotational motion of a single molecule, one can gain understanding of the molecular potential-energy surface, the associated electronic and vibrational excitations, and the coupling of electrons to nuclear motion. By studying single molecules, it is possible to determine local environmental effects. Current interest in single atom–molecule manipulation is due in part to the possibility that the reversible motion of individual atoms and molecules will ultimately be used in memory or electromechanical devices. Although not a practical device, the reversible rotation of a single diatomic molecule is a demonstration of this concept.

REFERENCES AND NOTES

1. D. M. Eigler, C. P. Lutz, W. E. Rudge, *Nature* **352**, 600 (1991).
2. B. C. Stipe, M. A. Rezaei, W. Ho, *Phys. Rev. Lett.* **79**, 4397 (1997).
3. J. A. Stroscio and D. M. Eigler, *Science* **254**, 1319 (1991).
4. Ph. Avouris, *Acc. Chem. Res.* **28**, 95 (1995).
5. D. M. Eigler and E. Schweizer, *Nature* **344**, 524 (1990).
6. M. F. Crommie, C. P. Lutz, D. M. Eigler, *Science* **262**, 218 (1993).
7. T. A. Jung, R. R. Schlittler, J. K. Gimzewski, H. Tang, C. Joachim, *ibid.* **271**, 181 (1996).
8. L. Bartels, G. Meyer, K.-H. Rieder, *Phys. Rev. Lett.* **79**, 697 (1997).
9. Y. W. Mo, *Science* **261**, 886 (1993).
10. J. L. Gland, B. A. Sexton, G. B. Fisher, *Surf. Sci.* **95**, 587 (1980).
11. H. Steininger, S. Lehwald, H. Ibach, *ibid.* **123**, 1 (1982).
12. C. Puglia et al., *ibid.* **342**, 119 (1995).
13. B. C. Stipe et al., *Phys. Rev. Lett.* **78**, 4410 (1997).
14. B. C. Stipe, M. A. Rezaei, W. Ho, *J. Chem. Phys.* **107**, 6443 (1997).
15. A. Eichler and J. Hafner, *Phys. Rev. Lett.* **79**, 4481 (1997).
16. G. P. Salam, M. Persson, R. E. Palmer, *Phys. Rev. B* **49**, 10655 (1994).
17. S. Gao, M. Persson, B. I. Lundqvist, *ibid.* **55**, 4825 (1997).
18. This research was supported by the National Science Foundation under grant DMR-9417866. We thank M. Persson for comments and suggestions.

9 December 1997; accepted 5 February 1998